chemosensors

MDPI

Article

Influence of Nitrogen-Doped Carbon Dot and Silver Nanoparticle Modified Carbon Paste Electrodes on the Potentiometric Determination of Tobramycin Sulfate: A Comparative Study

Nermine V. Fares [1], Passant M. Medhat [2], Christine M. El Maraghy [2], Sherif Okeil [1,3,*] and Miriam F. Ayad [1]

[1] Analytical Chemistry Department, Faculty of Pharmacy, Ain Shams University, Abbassia, Cairo 11566, Egypt; dr.nermine@pharma.asu.edu.eg (N.V.F.); dr.miriamayad@pharma.asu.edu.eg (M.F.A.)
[2] Analytical Chemistry Department, Faculty of Pharmacy, October University for Modern Sciences and Arts (MSA), 6th of October City 11787, Egypt; pmedhat@msa.eun.eg (P.M.M.); christine_elmaraghy@hotmail.com (C.M.E.M.)
[3] Institute for Particle Technology and Laboratory for Emerging Nanometrology, Technische Universität Braunschweig, Volkmaroder Str. 5, 38104 Braunschweig, Germany
* Correspondence: s.okeil@tu-braunschweig.de or sherif_okeil@hotmail.com

Abstract: Two inexpensive and simple methods for synthesis of carbon nanodots were applied and compared to each other, namely a hydrothermal and microwave-assisted method. The synthesized carbon nanodots were characterized using transmission electron microscopy (TEM), ultraviolet-visible (UV-Vis), photoluminescence (PL), Fourier transform-infrared spectroscopy (FTIR), and X-ray diffraction (XRD). The synthesized microwave carbon nanodots had smaller particle size and were thus chosen for better electrochemical performance. Therefore, they were used for our modification process. The proposed electrodes performance characteristics were evaluated according to the IUPAC guidelines, showing linear response in the concentration range 10^{-6}–10^{-2}, 10^{-7}–10^{-2}, and 10^{-8}–10^{-2} M of tobramycin with a Nernstian slope of 52.60, 58.34, and 57.32 mV/decade for the bare, silver nanoparticle and carbon nanodots modified carbon paste electrodes, respectively. This developed potentiometric method was used for quantification of tobramycin in its co-formulated dosage form and spiked human plasma with good recovery percentages and without interference of the co-formulated drug loteprednol etabonate and excipients.

Keywords: carbon paste electrode; carbon nanodots; silver nanoparticles; hydrothermal and microwave assisted methods; tobramycin sulfate

Citation: Fares, N.V.; Medhat, P.M.; El Maraghy, C.M.; Okeil, S.; Ayad, M.F. Influence of Nitrogen-Doped Carbon Dot and Silver Nanoparticle Modified Carbon Paste Electrodes on the Potentiometric Determination of Tobramycin Sulfate: A Comparative Study. *Chemosensors* **2021**, *9*, 52. https://doi.org/10.3390/chemosensors9030052

Academic Editor: Tatsuo Yoshinobu

Received: 14 February 2021
Accepted: 4 March 2021
Published: 7 March 2021

1. Introduction

Tobramycin sulfate (TOBRA) is a broad-spectrum aminoglycoside antibiotic (Figure S1), produced by *Streptomyces tenebrarius* [1]. It is highly effective against gram-positive and gram-negative bacteria, especially pseudomonas species. Although antibiotics are only directed against bacteria and not viruses, the aminoglycoside class of antibiotics, to which tobramycin belongs, could be used for treatment of secondary bacterial infections which could accompany the viral COVID-19 pneumonia [2]. Moreover, it was found that COVID-19 patients had symptoms of conjunctivitis [3], which can be treated with TOBRA. It was found that upon TOBRA administration as ophthalmic eye drops, some systemic absorption occurs, and the mean peak serum level reaches C_{max}= 5 µg/mL [4]. Therefore, it was an urgent need to find a fast and sensitive method for quantification of TOBRA in human plasma, because the drug not only exerts its effects in the organ treated, but can in fact also evoke systemic harmful effects, namely headache and laryngospasm, when TOBRA is absorbed into the circulation, which requires careful monitoring [5].

However, the analysis of TOBRA is complicated, as it lacks absorbing chromophore and fluorophore groups in its structure (Figure S1), so it cannot be easily measured using

spectroscopic techniques. Additionally, it is a highly polar molecule, having weak retention on reversed-phase liquid chromatographic columns, and its extraction is hindered by its high polarity [6]. These properties make TOBRA difficult to analyze. Chromatographic [6] and spectroscopic [7] methods have been reported for the determination of TOBRA using various derivatizing agents, but these methods have disadvantages of being tedious and time-consuming due to derivatization steps.

Potentiometric methods have several advantages, such as being green with no excessive solvent consumption, simple, sensitive, and fast, and not requiring tedious sample pretreatment steps [8]. While there are different forms of potentiometric electrodes, carbon paste electrodes, being all-solid-state electrodes, are of special interest, as they possess large potential windows, low background current, chemical inertness, low cost, surface renewability, and no need for an internal filling solution [9]. Furthermore, they are easily miniaturized and enable on-site analysis. They are composed of graphite powder, an electroactive material, and a liquid binder, with the addition of nanoparticles as a new modification [9]. A literature survey revealed that electrochemical determination of TOBRA was mainly performed through voltammetric sensors [10–12], and to date there is only one potentiometric sensor for the direct determination of TOBRA through a classical ion-selective electrode, where the sensing membrane was composed of β-cyclodextrin as ionophore for the evaluation of permeability of TOBRA in gram-negative bacteria [13]. Additionally, no carbon paste electrodes, whether bare or modified with nanoparticles, have been used for electrochemical determination of TOBRA.

Modification of the electrode sensing cocktail is a highly crucial issue, as it enables the fine tuning of the sensor response towards the target analyte, thus increasing the sensitivity and selectivity of the electrode [14]. Taking a look in the literature, carbon paste electrodes are modified through various nanomaterials, which usually offer an increased sensitivity. This is due to the increased surface area and fast response rate owing to the enhanced electron-transfer kinetics and reduced resistance [15–17]. One class of nanomaterials is metallic nanoparticles, which have attracted great attention due to their variety of applications in fields of biomedical optical and electrical sensing, resulting in the fabrication of many sensors for the detection of various analytes [18,19]. An example of the metallic nanoparticles is silver nanoparticles (AgNp). They are noble metal nanoparticles that have a particle size between 1–100 nm and possess unique optical, electronic, and antibacterial properties and high conductivity and are widely used in different areas such as bio-sensing, photonics, and antimicrobial and medical applications [18,20]. Silver nanoparticles have been mainly used in electrochemical sensors due to their high conductivity and high electrocatalytic activity, which are interesting properties, especially for voltammetry-based methods [18]. They have been used as additives to improve the sensitivity and selectivity of electrochemical sensors by signal amplifications and the conversion of chemical signal to electrical response, thus increasing the sensitivity of the proposed electrodes [21].

At the same time, there has been a lot of work investigating the inclusion of carbon nanomaterials in potentiometric sensors [22]. However, to date very little work has been performed on investigating the influence of modification of electrochemical sensor in general and potentiometric sensors in particular with carbon nanodots (C-dots) and especially doped C-dots on the electrochemical sensor performance in terms of sensitivity, selectivity, response time, etc. [23,24]. C-dots are the newest member of carbon-based nanomaterial family. C-dots are amorphous carbon nanoparticles with particle size ranging from 1–10 nm.

Preparation approaches of C-dots include two main techniques, "top-down" and "bottom-up" approaches. The "top-down" synthetic route involves cutting large carbon structures such as graphite and carbon nanotubes into C-dots using laser ablation and electrochemical methods. However, the "bottom-up" synthetic route involves the synthesis of C-dots from small molecules as precursors such as carbohydrates, citrates, and polyaromatic hydrocarbons. This "bottom-up" technique could be done by many methods such as hydrothermal, microwave-assisted method, pyrolysis, and ultrasonic and acid dehy-

dration methods. Additionally, recent studies reported emerging, low cost raw materials used in the preparation of C-dots applied in electrochemical sensors such as biomasses and biochar [25,26], which shows the variety of starting materials that can be used for C-dot synthesis.

The most widely used techniques for C-dots synthesis are the hydrothermal and the microwave-assisted methods because of their relatively low cost and easy operating steps. However, the microwave-assisted method is considered to be greener, faster, and simpler for C-dots synthesis as compared to the hydrothermal one [27,28]. However, microwave-assisted synthesis became the most popular one because the synthesis process is completed in one step and consequently, it is quick and easy.

C-dots have been mainly used for optical sensors [27] due to their extraordinary fluorescence and quantum yield, but at the same time, they possess interesting conductive properties besides their interesting surface functionalization, which can be tuned depending on the starting materials and synthesis process, which makes them highly interesting candidates for electrochemical sensors. They have attracted great interest in sensor fabrication due to their large surface area, high sensitivity, mechanical strength, and selectivity to the target ion, and also good electrocatalytic activity. They have sp^2 and sp^3 hybridized carbon atoms with several OH, NH_2, and COOH functional groups on their surface, which are responsible for their durability and excellent solubility in the sensing cocktail [27,28].

Recently, an interesting work was published comparing the effect of doping in C-dots on the performance of electrochemical sensors [24], showing the advantages of using doped C-dots for electrochemical determinations. However, C-dots were still incorporated in sensors for voltammetric and not potentiometric determination of analytes [23,24,29,30]. Therefore, it would be interesting to investigate the effect of C-dots on potentiometric sensors and to put it in a bigger picture through comparing it with noble metal nanoparticles such as modifiers, which were frequently used in literature for modification of electrochemical sensors.

Thus, in the presented work, two types of nanoparticles were incorporated into our constructed carbon paste sensors; the first one is AgNp and second is C-dots synthesized by two methods (hydrothermal and microwave-assisted methods). Electrochemical performance of the synthesized sensors was evaluated and compared to study the effect of nanoparticle addition. The developed sensors were successfully applied for quantitative determination of TOBRA in its co-formulated pharmaceutical dosage form without interference from loteprednol etabonate and excipients. TOBRA was further determined in spiked human plasma without interference from matrix components.

2. Materials and Methods

2.1. Instrumentation and Characterization

For the potentiometric measurements, a Ag/AgCl double junction electrode (Sigma-Aldrich, St. Louis, MO, USA) serving as an external reference electrode containing AgCl saturated with 0.3 M KCl as an inner filling solution was used and connected to Jenway digital ion analyzer Model3505 (Bibby Scientific Ltd., Stone, UK). pH adjustments were performed with a potentiometer using a Jenway pH glass electrode Model P14/BNC (Bibby Scientific Ltd., Stone, UK).

The hydrothermal synthesis of C-dots was performed using a Teflon-lined stainless-steel autoclave, while in the microwave synthesis of C-dots, a domestic microwave oven with 750 W (LG electronics, Tokyo, Japan) was used. Centrifugation of the synthesized C-dots dispersion was performed using a Sigma Centrifuge (model no. D-37520 Osterode am Harz, Göttingen, Germany) and the dispersion of the C-dots was done using an Elma Schmidbauer GmbH sonicator (model S30H, Singen, Germany).

The synthesized C-dots were visualized by transmission electron microscopy (TEM) using JEOL JEM-1400 electron microscope (Jeol Ltd., Tokyo, Japan) at 80 kV. X-ray diffraction (XRD) was performed on a Bruker AXS (D8 Advance), USA, using Cu Kα1 radiation (λ = 1.541 Å). Analysis of the surface functional groups of the C-dots was performed using

a Perkin Elmer Fourier transform infrared spectrometer (FTIR), USA. A double beam spectrophotometer (UV-1800, Shimadzu-Japan) was used to record the UV spectra using 4 cm quartz cell, and a personal computer having UV-probe 2.10 software was connected. A spectrofluorimeter (Shimadzu, Japan) was used for fluorescence measurements using 1 cm quartz cell and a personal computer with Cary Eclipse scan application version 1.2. The total nitrogen (TN) content in nitrogen-doped C-dots was determined by a Multi N/C 3100 analyzer (Analytik Jena, Jena, Germany).

2.2. Materials

2.2.1. Samples

Pure Sample

TOBRA of purity 100.74% ± 0.505 according to reference method [7] was purchased from Al Andalous for Pharmaceutical Industries (Giza, Egypt).

Pharmaceutical Formulation

Lotepred® T ophthalmic solution (batch no. FTS0031) manufactured by Akums Drugs & Pharmaceuticals Ltd., labeled to contain 3000 µg TOBRA per 1 mL, was purchased from a local pharmacy.

2.2.2. Reagents

All chemicals used throughout this work were of analytical grade, and all solvents were of spectroscopic grade. Water was double distilled by Automatic Water still (Sci Finetech, Seoul, Korea). Polyvinylpyrrolidone (PVP)-capped silver nanoparticles powder (<100 nm) and graphite powder (mesh size < 20 µm) were purchased from Sigma Aldrich, USA. Fresh human plasma was purchased from VACSERA (Cairo, Egypt). Tetrahydrofuran (THF) and phosphotungestic acid (PTA) were purchased from Alfa Aesar (Ward Hill, MA, USA).

Methanol was purchased from Fischer Scientific, USA. Paraffin oil, NaCl, $CaCl_2$, and glucose were purchased from El Nasr Company (Cairo, Egypt). Sucrose, orthophosphoric acid, citric acid, acetic acid, sodium hydroxide, and sodium dodecyl sulfate (SDS) were purchased from Loba Chemie, India. Boric acid and urea were obtained from Oxford Laboratory reagent, India. Benzalkonium chloride, Gentamicin, and Amikacin were kindly supplied by Rameda for pharmaceutical industries (Cairo, Egypt). Loteprednol Etabonate was kindly supplied by Al Andalous for pharmaceutical industries (Giza, Egypt).

Britton–Robinson buffer was prepared covering the pH range (2–12) following the procedure stated in the literature [31].

2.3. Standard Solutions

2.3.1. Standard Stock Solution

An appropriate weight of TOBRA reference material was accurately weighed and transferred into a 100 mL volumetric flask, and the volume was completed to the mark with Britton–Robinson buffer (pH 6.0) to prepare the first stock solution, having a concentration of 1×10^{-2} M.

2.3.2. Working Standard Solutions

Working standard solutions (1×10^{-10}–1×10^{-3} M) were prepared by accurately transferring aliquots from the prepared stock solution (1×10^{-2} M) into 100 mL volumetric flasks, and the volume was completed using Britton–Robinson buffer (pH 6.0).

2.4. Procedures

2.4.1. Preparation of C-Dots by Microwave-Assisted Method

C-dots of uniform particle size were successfully prepared using citric acid and urea by microwave-assisted method described by Wang et al. [32]. In short, citric acid was dissolved with an equal weight of urea in distilled water, and the clear solution was heated in a domestic microwave for 5 min at a power of 750 W. The obtained dark brown solid

was heated in a vacuum-oven for about 1 h at 60 °C, followed by dissolving the product in distilled water, centrifugation at 3000 rpm for 20 min, and filtration through a 0.25 µm syringe filter in order to get rid of large particles and agglomerates. The resultant brownish dispersion was then dried in an oven at 60 °C overnight, and the obtained solid could be then dispersed through sonication in the solvent of choice.

2.4.2. Preparation of C-Dots by Hydrothermal Method

Hydrothermal synthesized C-dots were prepared using sucrose and NaOH in Teflon-lined stainless-steel autoclave according to the method described by Lee et al. [33]. In short, sucrose was dissolved together with NaOH in an appropriate amount of water and the clear, transparent solution was heated in a Teflon-lined stainless-steel autoclave at 160 °C for 4 h. The resulting dispersion was cooled down, centrifuged at 3000 rpm for 20 min, and filtered through a 0.25 µm syringe filter to remove any big particles or by-products. The obtained solution was heated at 100 °C to precipitate any unreacted NaOH, which was then removed by filtration to obtain an aqueous C-dots dispersion.

2.4.3. Preparation of the Ion-Pair

The ion pair of TOBRA-PTA was prepared by slowly mixing 50 mL of 10^{-2} M PTA with 50 mL 10^{-2} M TOBRA, through stirring for 10 min. The resulting white precipitate was left in the mother liquor for 24 h to coagulate. Then, it was filtered through a filter paper and was allowed to dry at room temperature to be finally ground to a fine powder.

2.4.4. Sensors Fabrication

Bare Carbon Paste Electrode (Bare-CPE)

Twenty milligrams of TOBRA-PTA ion pair was mixed with 300 mg graphite powder in a mortar. The ion pair and the graphite powder were homogenized with few drops of liquid paraffin to form a smooth paste. The paste was then packed into a plastic tube (4 mm in diameter) to prevent air gaps formation. The electrical contact was established by inserting a copper wire (2 mm in diameter). A sandpaper was used to polish and smooth the external surface of the electrode. Finally, the electrode was conditioned by soaking into 10^{-2} M TOBRA solution for 24 h before use.

Silver Nanoparticles Modified Carbon Paste Electrode (AgNp-CPE)

AgNp-CPEs were prepared by adding different weights of silver nanoparticles powder ranging from (3–40 mg), while keeping the amounts of graphite powder, ion pair, and paraffin oil unchanged. AgNp-CPE was prepared by the same procedure as mentioned in the Bare-CPE preparation. The electrode was conditioned by soaking it in 10^{-2} M TOBRA solution for 24 h before use.

C-Dots Modified Carbon Paste Electrode (C-Dots-CPE)

C-dots-CPEs of different C-dots content were prepared by suspending 1 mg of C-dots powder into 350 µL THF through sonication for 30 min. From this dispersion, different volumes ranging from (10–40 µL) were added to the bare carbon paste mixture. C-dots CPE were prepared by the same manner as mentioned in the Bare-CPE preparation. The electrode was conditioned by soaking in 10^{-2} M TOBRA solution for 24 h before measurement.

2.4.5. Potentiometric Cell—Assembly

Unmodified and modified carbon paste electrodes | TOBRA solution || Ag/AgCl, KCl (saturated solution)

2.4.6. Electrodes Calibration

After conditioning, the three constructed electrodes were separately immersed in each of the standard TOBRA solutions (1×10^{-10}–1×10^{-2} M) in conjunction with the double junction Ag/AgCl reference electrode. The electromotive force (emf) within ±1 mV was

measured and recorded. The electrodes were well washed with distilled water between the runs to reach a constant potential. To obtain a fresh surface of the paste, the paste was squeezed out, and the surface was polished with a filter paper. The emf was plotted against the logarithm of the prepared TOBRA concentrations.

2.4.7. Application to Pharmaceutical Formulation

To determine TOBRA in its pharmaceutical dosage form, different aliquots of Lotepred® T ophthalmic solution were transferred separately into 25 mL volumetric flasks, and then the volume was completed to the mark using Britton–Robinson buffer pH 6.0 to obtain final concentration of 1×10^{-5}, 1×10^{-4} and 1×10^{-3} M of TOBRA. The three prepared electrodes were immersed in the three prepared solutions, along with the double junction Ag/AgCl reference electrode. The emf was recorded, and the concentration was calculated from the corresponding regression equation accordingly.

2.4.8. Application to Spiked Human Plasma

To prepare the samples, three 20 mL stoppered shaking test tubes were loaded with different aliquots of TOBRA stock solutions, 1 mL plasma, and 2 mL methanol. The tubes were shaken for 1 min before being centrifuged at 8000 rpm for 30 min. To prepare 1×10^{-6}, 1×10^{-5} and 1×10^{-4} M TOBRA plasma solutions, the supernatant was transferred into three 25 mL volumetric flasks and diluted with Britton–Robinson buffer, pH 6.0. The three prepared electrodes were immersed in the spiked plasma solutions along with the reference electrode and then washed with water in between measurements. The emf of each solution was measured by the proposed electrodes, and the concentration of TOBRA was determined using the corresponding regression equation.

3. Results and Discussion

3.1. Characterization of the Synthesized C-Dots

The success of C-dots synthesis was proved using various characterization techniques. The morphology of both microwave and hydrothermally-synthesized C-dots was characterized by TEM, as shown in Figure 1a,b, respectively. In case of the former method, TEM image showed that C-dots are spherical in shape, dispersed, and uniform in aqueous solution with a particle size less than 10 nm, while the hydrothermally-synthesized C-dots were spherical with a particle size ranging from 80 to 160 nm. Moreover, the TEM image of the hydrothermally synthesized C-dots shows several grey patches (Figure 1b), which is most probably due to organic by-products, which could be formed during the hydrothermal synthesis. It is known that microwave-assisted methods are quicker and more selective, resulting in fewer by-products [34]. Since the microwave-synthesized C-dots have no apparent by-products, smaller particle size, and a higher monodispersity compared to the hydrothermal synthesized ones, higher electro-active surface area, increased conductivity, and electrochemical performance is expected. Therefore, they were subjected to further characterization and were chosen to be used in later steps for modification of the bare carbon paste electrode to evaluate its electrochemical performance.

The optical properties of the nanoparticles were revealed using UV-Vis spectrophotometry and spectrofluorimetry. In UV-Vis spectrophotometry, the obtained spectrum (Figure 2a) showed three peaks at 405, 340, and 272 nm. The peak placed at 272 nm is a usual characteristic of C-dots and is due to $\pi \rightarrow \pi^*$ transition of carbon nanoparticles [35,36]. The peak at 340 nm arises from $n \rightarrow \pi^*$ transition of the C = O bond, and the peak at 405 is due to the extended conjugation found in C-dots structure [32,37]. The fluorescence spectrum (Figure 2b) showed an emission peak at 524 nm after being excited at 420 nm, representing green fluorescence.

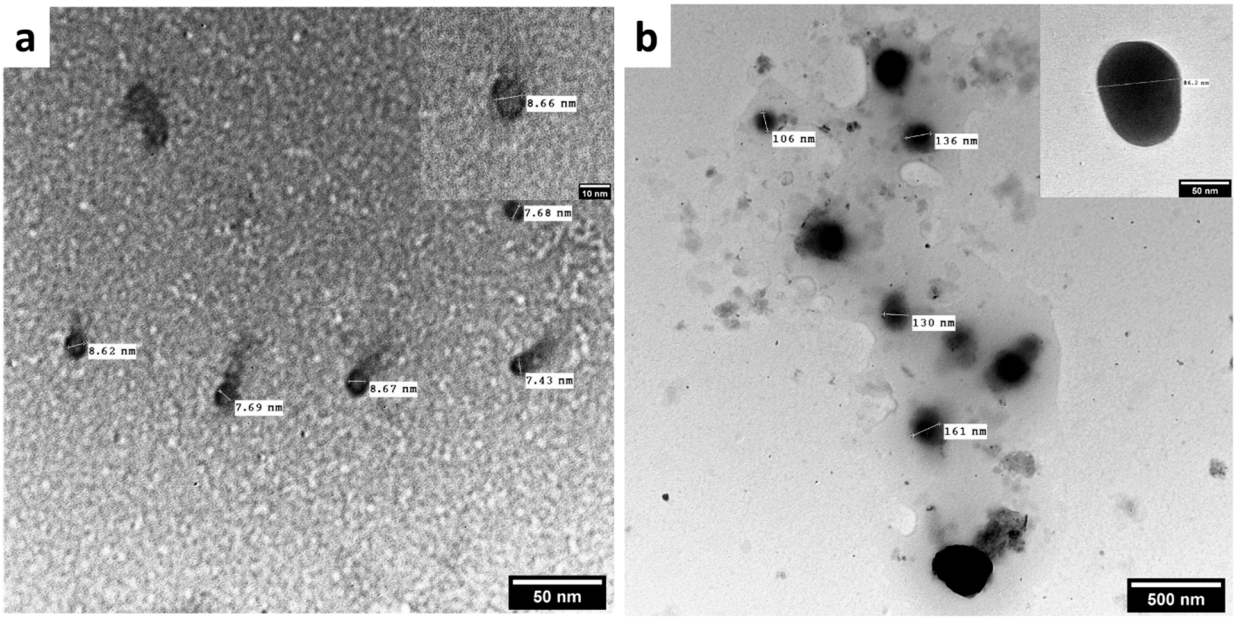

Figure 1. TEM image of (**a**) microwave-synthesized C-dots, (**b**) hydrothermally synthesized C-dots. In each inset, a single particle can be seen.

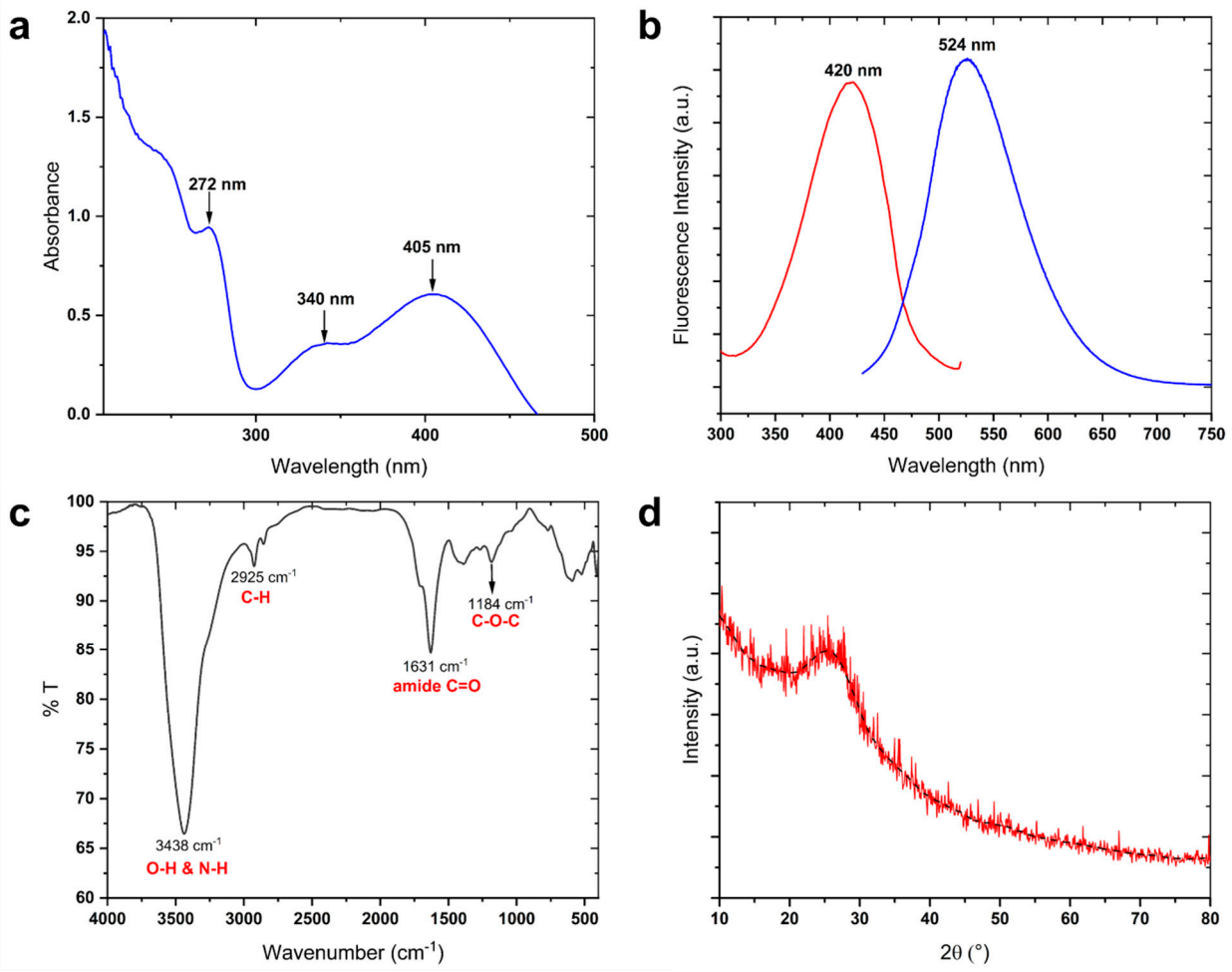

Figure 2. (**a**) UV-Vis spectrum of the microwave-synthesized C-dots showing three peaks at 405, 340, and 272 nm, (**b**) fluorescence spectrum of the microwave-synthesized C-dots showing excitation and emission peaks at 420 and 524 nm, respectively, (**c**) FTIR of the microwave-synthesized C-dots, and (**d**) XRD pattern of the microwave-synthesized C-dots.

The carbonyl, hydroxyl, and amine groups, which are characteristic functional groups on the surface of the C-dots, were characterized by FTIR (Figure 2c), where the broad absorption band at 3438 cm^{-1} is attributed to stretching vibration of O-H and secondary amine groups (N-H) [35]. These groups improve the dispersibility of the C-dots in sensing cocktail and avoid agglomerates formation. The C=O stretching vibration band appears at 1631 cm^{-1} and is an indication on an amide (-CONH-). Asymmetric and symmetric stretching vibrations of C-O-C appearing at 1100–1300 cm^{-1} point toward the presence of different oxygen-containing functional groups. The three peaks appearing at 1268, 1390, and 2925 cm^{-1} are characteristic to C-C, C=C, and C-H stretching vibrations, respectively, proving the presence of alkyl and aryl groups [32,35]. In order to prove the nitrogen doping, the total nitrogen content was determined in the microwave-synthesized C-dots, where a suspension of nitrogen-doped C-dots with a concentration of 208 μg/mL revealed a total nitrogen concentration of 29.98 μg/mL, which means a nitrogen content of about 14.4%, proving the presence of a considerable amount of nitrogen in these nitrogen-doped C-dots.

The XRD pattern shown in (Figure 2d) reveals a broad peak at $2\theta = 27^{\circ}$, which is characteristic to the mainly amorphous nature of the synthesized C-dots [32,38].

3.2. Electrodes Fabrication

This method is based on coupling the cationic TOBRA with an anionic exchanger PTA, since TOBRA has a basic character (pK_a = 8.4) [39], so that at acidic pH, the amino group is protonated and acts as a cationic exchanger. The cationic TOBRA was found to form an insoluble ion-pair with PTA in the ratio 1:1, as proven by the Nernstian slopes obtained.

Optimization of the Modified CPE Composition

The linearity, sensitivity, and selectivity of the electrodes depend on their composition. The modified carbon paste electrodes had the same composition as the bare carbon paste electrode (the amount of the graphite powder and ion pair are constant) with addition of ten different amounts of AgNp nanoparticles (3–40 mg), as shown in Figure S2a, or fourteen different C-dots suspension volumes ranging from 10–40 μL, Figure S2b. It is important to disperse the C-dots in an appropriate solvent in order to enable good dispersion of the C-dots on one hand and to ensure good mixing and miscibility with the other membrane components on the other hand to ensure equal distribution of the C-dots within the sensing cocktail without aggregation for optimal sensor performance. For that, THF and an aqueous SDS solution were investigated, where the C-dots were dispersed through sonication before mixing the dispersion with the other sensing cocktail components as done with other carbon materials in literature [40,41]. The C-dots dissolved in aqueous SDS solution resulted in low slopes and gave non-reproducible results when incorporated into the sensing cocktail, which is most probably a result of inadequate mixing of the SDS-based solution with the other components, resulting in inhomogeneous sensing cocktails. According to the obtained results, the electrode composed of 4.5 mg AgNp and that with 15 μL C-dots suspension dissolved in THF were found to be optimal for the determination of TOBRA, as they showed the best slope values of 58.34 and 57.32, respectively. Therefore, these two modified electrodes were selected for further experiments. It was found that mixing nanoparticles in the carbon paste increased the electro-active surface area and improved the conversion of chemical signal to electrical response and hence increased the conductivity and the sensitivity of the proposed electrodes. The addition of higher amounts of nanoparticles lead to a potential decrease of the slope and non-reproducible results, which probably resulted from reduction of the catalytic properties of electron transfer and the increase of the charge transfer resistance upon addition of higher amounts of nanoparticles [42].

3.3. Optimization of the Working pH

The pH adjustment of the measured solution is a critical step in the functioning of the fabricated electrodes. Therefore, the effect of pH on the response of the proposed electrodes

was studied. As shown in Figure 3, the potential of the proposed electrodes was almost stable in solutions of pH values 5.5–7.5. This could be attributed to the ionization of TOBRA at acidic pH, being a basic drug with an average pK_a value of 8.4. It was found that there would be approximately 9% rise in the TOBRA charged fraction as pH declined from 7.4 to 6.4 (that is, 90% charged to 99% charged) [39]. Consequently, a Britton–Robinson buffer of pH = 6 was chosen to be the best working pH value for the three proposed electrodes where the sensors responses were stable. The changes in potential at higher and lower pH values are due to H^+ and OH^- interference, as they are present at higher concentrations than the target ion. Moreover, at high pH values above 8, the potential decreased, probably due to the decrease of the ionized fraction of the drug from 90%, reaching 50% only [39].

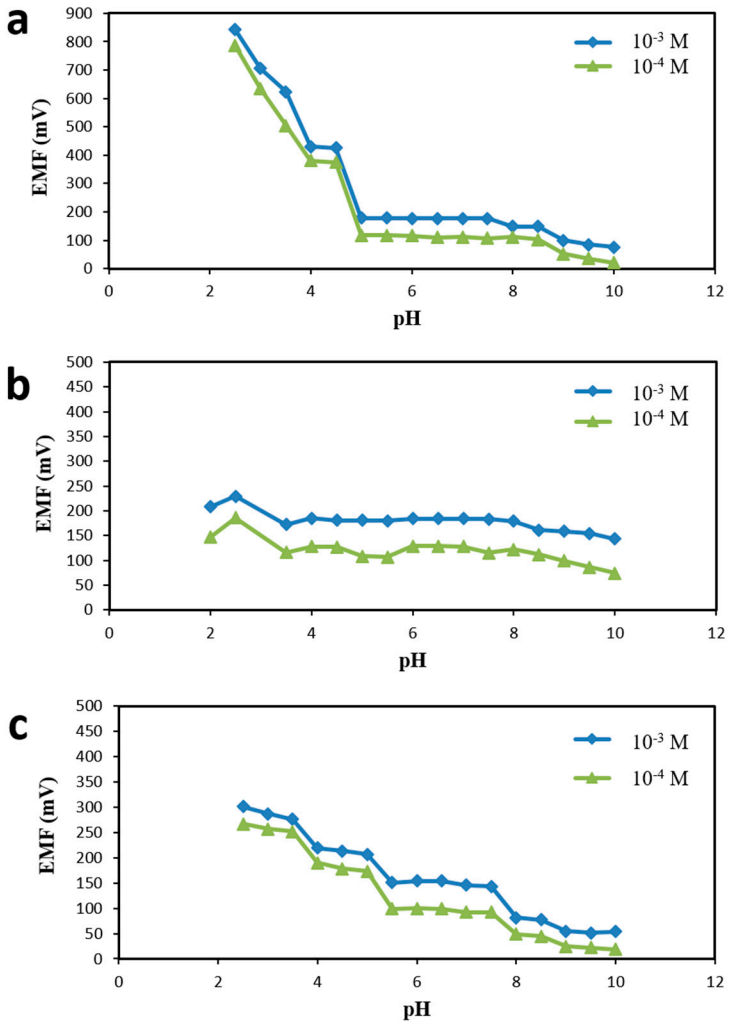

Figure 3. Effect of pH on the response for the proposed (**a**) Bare-Carbon paste electrode, (**b**) AgNp-modified Carbon paste electrode, and (**c**) C-dots-modified Carbon paste electrode using 1×10^{-3} and 1×10^{-4} M TOBRA concentration.

3.4. Performance Characteristics of the BARE-CPE, AgNp-CPE, and C-Dots-CPE

The electrochemical performance of the proposed electrodes was evaluated according to IUPAC recommendation guidelines [43]. The proposed electrodes exhibited cationic Nernstian slopes with sensitivity depending on the electrode composition, as shown in Table 1. C-dots modified CPE was the most sensitive when compared to other electrodes, with detection limit down to 3.2×10^{-9} M, followed by AgNps modified CPE with detection limit 1.8×10^{-8} M and bare-CPE with the least sensitivity with a detection limit of 1.8×10^{-7} M. Slopes of the calibration curves were found to be 52.60, 58.34, and

57.32 mV/decade with linearity ranges 10^{-6}–10^{-2}, 10^{-7}–10^{-2}, and 10^{-8}–10^{-2} M for bare, AgNp, and C-dots modified CPE, respectively (Figure 4).

Table 1. Performance characteristics of the three fabricated electrodes.

Parameters	Bare-CPE	Ag-Np-CPE	C-dots-CPE
Slope (mV/decade)	52.60	58.34	57.32
Intercept	605.00	484.20	522.46
LOD [a] (M)	1.8×10^{-7}	1.8×10^{-8}	3.2×10^{-9}
Response time (s)	30	10	10
Working pH range	5–7.5	3.5–8	5.5–7.5
Concentration range (M)	10^{-6}–10^{-2}	10^{-7}–10^{-2}	10^{-8}–10^{-2}
Stability/Lifetime (days)	21 days	28 days	36 days
Accuracy [b] (mean recovery ± SD)	100.35 ± 1.002	99.77 ± 0.947	99.88 ± 1.239
R	0.9999	0.9999	0.9999
Intra-day precision (RSD%) [c]	0.756	0.601	0.544
Inter-day precision (RSD%) [c]	0.955	0.893	0.672

[a] LOD: Limit of detection is calculated by extrapolating the calibration curve linear segments. [b] Mean of five determinations. [c] Relative standard deviations for three concentrations (1×10^{-6}, 1×10^{-5}, 1×10^{-4} M) carried out in triplicate on the same day for intra-day precision and on three successive days for inter-day precision.

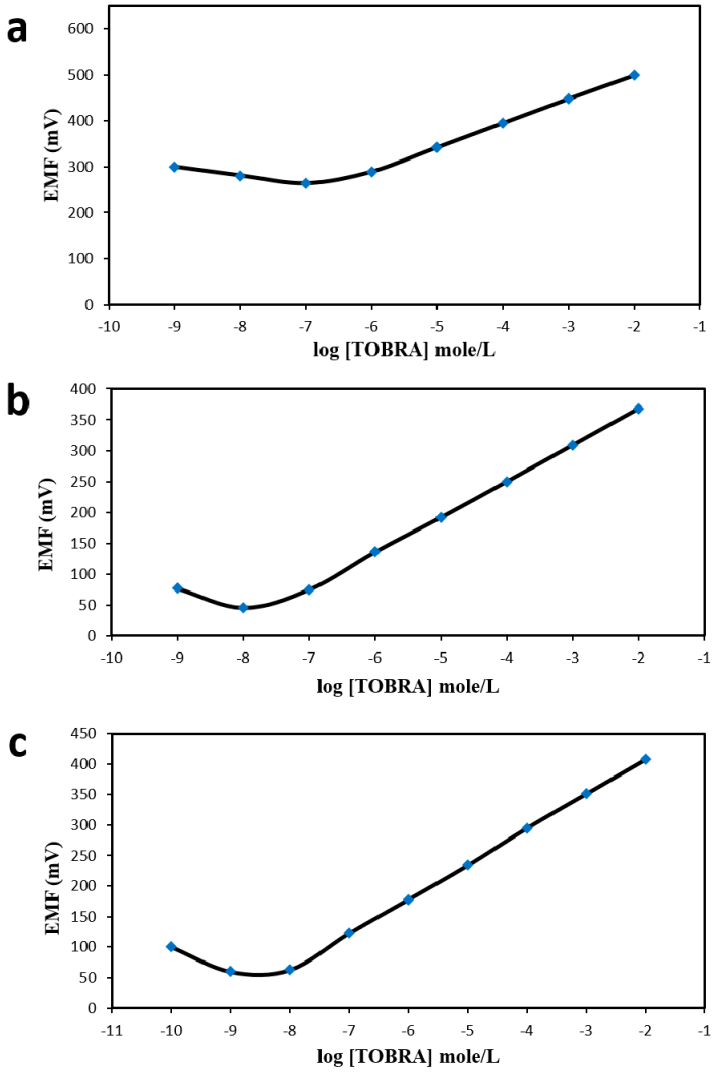

Figure 4. Calibration curves of (**a**) Bare-Carbon paste electrode, (**b**) AgNp-modified Carbon paste electrode, and (**c**) C-dots-modified Carbon paste electrode.

The response time is important, as it helps to analyze a large number of samples in a short time, and it was found that AgNp and C-dots modified CPEs had shorter response times compared to the Bare-CPE Table 1.

Comparing the performance of the C-dot modified CPE with AgNp-CPE and the Bare-CPE reveals that the C-dot modified CPE outperforms the other electrodes in terms of sensitivity and linear range, which can be attributed to its good conductivity, high surface area, and excellent adsorption properties of organic molecules due to its carbonic nature as well as its surface functional groups. Moreover, the modification of the sensing cocktail with nitrogen-doped C-dots provides an increased hydrophilicity due to the different surface functional groups, enabling an improved wetting and subsequently a better contact to aqueous solutions, which also results in an improved sensing. Furthermore, the C-dots-CPE possesses higher stability and has a short response time, which is comparable to the response time of AgNp-CPE. The prolonged lifetime of the electrode in case of AgNp when compared to the Bare-CPE is mainly a function of its antibacterial and antifouling properties [44]. Surprisingly, the lifetime of the C-dots-CPE was even longer than that of the AgNp-CBE, which indicates that the included C-dots also have interesting antifouling properties, as recently observed by several other works [45,46]. At the same time, several other reasons could be involved in leading to the increased stability in case of the C-dots-CPE, which need to be further investigated. All this shows that C-dots provide cheap alternatives to noble metal nanoparticles and can even outperform them in certain cases if it they are tailored for the specific application through the precursors and the synthesis process.

The proposed sensors were also compared with other electrochemical sensors from literature for determination of TOBRA [13,47], as shown in Table 2. This comparison shows that C-dots-CPE is superior to the reported aptamer-based gold sensor and β-Cyclodextrin-based sensor concerning the LOD, working pH range, lifetime, and intraday precision.

Table 2. Comparison of the sensors prepared in this work with other electrochemical sensors for the determination of TOBRA from literature.

Parameters	Bare-CPE	Ag-Np-CPE	C-Dots-CPE	Aptamer-Based Gold Sensor [47]	β-Cyclodextrin-Based Sensor [13]
Technique	Potentiometry			Differential pulse voltammetry	Potentiometry
Intercept	605.00	484.20	522.46	0.1334	389.3
LOD [M] [a]	1.8×10^{-7} [a]	1.8×10^{-8} [a]	3.2×10^{-9} [a]	5.13×10^{-9} [b]	1×10^{-6} [a]
Working pH range	5–7.5	3.5–8	5.5–7.5	7–7.5	5.5–7.5
Concentration range	10^{-6}–10^{-2} M	10^{-7}–10^{-2} M	10^{-8}–10^{-2} M	10–200 nM	10^{-5}–10^{-2} M
Stability/Lifetime (days)	21 days	28 days	36 days	14 days	21 days
R	0.9999	0.9999	0.9999	0.9969	0.998
Intra-day precision (RSD%)	0.756	0.601	0.544	4.3	2.74

[a] LOD: Limit of detection is calculated by extrapolating the calibration curve linear segments. [b] LOD: (3×standard deviations of blank signal/sensitivity).

3.5. Selectivity of the Proposed Electrodes

Selectivity of an ion selective electrode is defined as its specificity towards the target ion, in presence of other interfering ions present in the solution. The matched potential method (MPM) was used to determine the selectivity coefficients of our proposed electrodes [48]. According to IUPAC, $K^{pot}_{A,B}$ can be calculated using the following equation:

$$K^{pot}_{A,B} = \frac{a'_A - a_A}{a_B} \quad (1)$$

where a'_A is the activity of the primary ion, a_A is the activity of the reference solution of the primary ion, and a_B is the activity of the interfering ion. Table 3 shows the values of $K^{pot}_{A,B}$ of

the proposed electrodes. Results proved high selectivity of the proposed electrodes towards TOBRA in the presence of other interferents such as inorganic anions, cations, co-formulated loteprednol etabonate, and additives as NaCl, $CaCl_2$, and benzalkonium chloride used in the pharmaceutical formulation. C-dots-CPE showed the best selectivity results for most of the tested interferents. Also interesting is the increased selectivity observed with similar aminoglycoside antibiotics (gentamicin and amikacin) as interferents, which shows the unique sensor characteristics achieved upon inclusion of nitrogen doped C-dots in the sensing cocktail.

Table 3. Selectivity coefficients ($K^{pot}_{TOBRA,\ interferent}$) of the three proposed CPE using matched potential method (MPM).

Interferents	Bare-CPE	AgNp-CPE	C-Dots-CPE
NaCl	1.24×10^{-2}	9.00×10^{-3}	6.68×10^{-3}
$CaCl_2$	1.75×10^{-1}	5.08×10^{-3}	9.00×10^{-3}
Benzalkonium chloride	1.575×10^{-2}	3.79×10^{-3}	9.00×10^{-3}
Glucose	9.90×10^{-2}	5.51×10^{-3}	2.986×10^{-3}
Loteprednol Etabonate	1.60×10^{-2}	9.00×10^{-3}	4.669×10^{-3}
Gentamicin	1.72×10^{-1}	3.028×10^{-2}	9.441×10^{-3}
Amikacin	3.15×10^{-1}	2.65×10^{-2}	8.66×10^{-3}

3.6. Water-Layer Test

The water-layer test was first introduced by Fibbioli et al. [49] to test the potential stability of solid-contact ion selective electrodes such as carbon paste electrodes. This test was performed by recording the potential of the electrode in a solution containing the primary ion (1×10^{-5} M) TOBRA for one hour, then in a solution containing an interfering ion (0.1 M NaCl) for one hour, and then changing back to the TOBRA solution again.

As shown in Figure S3, the Bare-CPE showed negative drift in the interfering ion solution and positive potential drift when returned into TOBRA solution, which suggested the presence of a water layer. On the contrary, there were emf changes of approximately 100 mV upon switching the solutions from (1×10^{-5} M) TOBRA to 0.1 M NaCl in case of the AgNp and C-dots modified CPEs, which is due to change in the phase boundary potential at the interface between CPE and the sample, thus proving the sensing cocktail selectivity with a stable potential upon returning the electrode back to the TOBRA solution, proving the absence of water layer on the surface of proposed carbon paste electrodes and the improvement of the potential stability after the addition of nanoparticle in the solid contact electrode.

3.7. Application of the Proposed Electrodes for Analysis of Lotepred® T Ophthalmic Solution and Spiked Human Plasma

The proposed sensors were used for the analysis of TOBRA in Lotepred® T ophthalmic solution and spiked human plasma. Results obtained in Table 4 revealed the good recovery percent of the proposed electrodes for quantification of TOBRA in its dosage form and human plasma without interference from the co-formulated drug (Loteprednol Etabonate) or any other excipients and matrix components.

Table 4. Determination of TOBRA in Lotepred® T ophthalmic solution and spiked human plasma by the proposed electrodes.

In Lotepred® T Ophthalmic Solution			
Taken TOBRA Conc (M)	**Bare-CPE**	**AgNp-CPE**	**C-Dots-CPE**
	Recovery%	**Recovery%**	**Recovery%**
$\mathbf{1 \times 10^{-5}}$	100.00%	101.00%	100.56%
$\mathbf{1 \times 10^{-4}}$	101.70%	100.00%	99.31%
$\mathbf{1 \times 10^{-3}}$	99.31%	99.20%	98.01%
Mean ±SD	100.34 ± 1.230	100.07 ± 0.902	99.29 ± 1.275
In Spiked Human Plasma			
Taken TOBRA Conc (M)	**Bare-CPE**	**AgNp-CPE**	**C-Dots-CPE**
	Recovery%	**Recovery%**	**Recovery%**
$\mathbf{1 \times 10^{-6}}$	100.80%	97.72%	99.44%
$\mathbf{1 \times 10^{-5}}$	97.94%	100.23%	97.46%
$\mathbf{1 \times 10^{-4}}$	99.31%	99.71%	97.72%
Mean ±SD	99.35 ± 1.430	99.22 ± 1.325	98.21 ± 1.076

3.8. Statistical Comparison

The statistical comparisons of the proposed methods and the reference method [7] for determination of TOBRA are shown in Table 5. Results revealed that there was no significant difference between the proposed and the published method in accuracy and precision, as the calculated t and F values were less than the theoretical ones.

Table 5. Statistical comparison between the proposed methods and the reference method [7] of TOBRA in its pure form.

Parameter	Bare-CPE	AgNp-CPE	C-Dots-CPE	Reference Method [7] [a]
Mean	100.35	99.77	99.88	100.74
SD	1.002	0.947	1.239	0.505
N	5	6	7	4
Variance	1.004	0.897	1.535	0.255
***t*-test**	0.703 (2.365) *	1.855 (2.306) *	1.303 (2.262) *	
F	3.937 (9.117) *	(9.013) *	6.02 (8.941) *	

* The parenthesis indicates the corresponding theoretical t and F values at ($p = 0.05$). [a] Colorimetric method where TOBRA reacts with diphenylamine to form a blue colored complex whose color intensity is measured at 635 nm.

4. Conclusions

In this study, two carbon paste electrodes modified with silver nanoparticles and nitrogen doped C-dots were fabricated and compared to a bare carbon paste electrode and were used for potentiometric determination of Tobramycin in bulk, co-formulated pharmaceutical dosage form, and spiked human plasma. Moreover, two methods for synthesis of C-dots, namely hydrothermal and microwave methods, were tried and compared. Microwave-synthesized C-dots had smaller particle size and a narrower particle size distribution than the hydrothermal ones and were thus used for the preparation of the C-dots-CPE.

The results of our experimental work revealed that the performance of the carbon paste electrode was highly improved by the addition of the nanoparticles to the paste. The newly proposed electrodes showed very wide linear dynamic response in the concentration range reaching 10^{-8}–10^{-2} M with excellent Nernstian slope reaching 58.34 mV/decade. C-dots-CPE was the most sensitive electrode with a LOD of 3.2×10^{-9} M with the best selectivity results. However, AgNp-CPE had the highest slope.

Nanoparticles in general have a positive effect on the performance of potentiometric electrodes due to their good conductivity and high surface area. While silver nanoparticles are interesting electrode modifiers due to their conducting and antifouling properties, doped carbon dots present a further interesting approach for potentiometric sensor modification further enhancing its sensitivity and stability. Furthermore, the ease of manufacture, low cost, and the ability to tune the surface functional groups and doping by selecting the appropriate starting materials enables a flexible tailoring of the carbon dots for the corresponding application, thus achieving high performance. Still more work is required to exploit the opportunities for the efficient incorporation of carbon dots in potentiometric sensors. Moreover, our proposed sensors were compared with other previously reported sensors for determination of TOBRA, showing several advantages regarding the limit of detection and lifetime.

Finally, it can be concluded that the modified CPEs had several advantages over the Bare-CPE ones, as they showed faster response time, longer life time, lower detection limit, wider linear dynamic range, and higher selectivity towards the target ion. Therefore, they are highly recommended for rapid and accurate routine quantitative analysis of TOBRA, especially during the COVID-19 pandemic.

Supplementary Materials: The following are available online at https://www.mdpi.com/2227-9040/9/3/52/s1: Figure S1: Chemical structure of Tobramycin sulfate, Figure S2: The effect of amounts of (a) AgNps (b) C-dots (dissolved in THF or SDS) on the electrochemical performance of modified CPEs using 0.3 gm graphite powder, 0.02 gm ion pair and 1 mL paraffin oil, Figure S3: Water layer test for (a) Bare-CPE, (b) AgNp-CPE and (c) C-dots-CPE.

Author Contributions: All authors contributed to this work as follows: conceptualization: N.V.F., C.M.E.M., and M.F.A.; experimental work: P.M.M.; data analysis and interpretation: N.V.F., P.M.M., C.M.E.M., S.O., and M.F.A.; Writing—Original draft preparation: P.M.M. and S.O.; Writing—Review and editing: S.O., N.V.F., M.F.A., and C.M.E.M.; supervision: N.V.F., C.M.E.M., and M.F.A. All authors have read and agreed to the published version of the manuscript.

Funding: This research received no external funding. We acknowledge support by the German Research Foundation and the Open Access Publication Funds of Technische Universität Braunschweig for covering the publication costs of this article.

Institutional Review Board Statement: Not applicable.

Informed Consent Statement: Not applicable.

Data Availability Statement: Not applicable.

Acknowledgments: The authors thank Modern Science and Arts University for providing the instruments to finish this work.

Conflicts of Interest: The authors declare no conflict of interest.

References

1. Dienstag, J.; Neu, H.C. In Vitro Studies of Tobramycin, an Aminoglycoside Antibiotic. *Antimicrob. Agents Chemother.* **1972**, *1*, 41–45. [CrossRef]
2. Nori, P.; Cowman, K.; Chen, V.; Bartash, R.; Szymczak, W.; Madaline, T.; Punjabi Katiyar, C.; Jain, R.; Aldrich, M.; Weston, G.; et al. Bacterial and fungal coinfections in COVID-19 patients hospitalized during the New York City pandemic surge. *Infect. Control Hosp. Epidemiol.* **2021**, *42*, 84–88. [CrossRef]
3. Chen, L.; Deng, C.; Chen, X.; Zhang, X.; Chen, B.; Yu, H.; Qin, Y.; Xiao, K.; Zhang, H.; Sun, X. Ocular manifestations and clinical characteristics of 535 cases of COVID-19 in Wuhan, China: A cross-sectional study. *Acta Ophthalmol.* **2020**, *98*, e951–e959. [CrossRef] [PubMed]
4. Wilhelmus, K.R.; Gilbert, M.L.; Osato, M.S. Tobramycin in ophthalmology. *Surv. Ophthalmol.* **1987**, *32*, 111–122. [CrossRef]
5. Vaajanen, A.; Vapaatalo, H. A Single Drop in the Eye-Effects on the Whole Body? *Open Ophthalmol. J.* **2017**, *11*, 305–314. [CrossRef] [PubMed]
6. Lai, F.; Sheehan, T. Enhancement of detection sensitivity and cleanup selectivity for tobramycin through pre-column derivatization. *J. Chromatogr. A* **1992**, *609*, 173–179. [CrossRef]
7. Mannan, A.; Asif, S.; Usmanghani, K. A Novel Sensitive Method for Quantitative Determination of Tobramycin by Spectrophotometer using Diphenylamine. *RADS J. Pharm. Pharm. Sci* **2017**, *5*, 37–42.

8. Hassan, A.K.; Ameen, S.T.; Saad, B. Tetracaine-selective electrodes with polymer membranes and their application in pharmaceutical formulation control. *Arab. J. Chem.* **2017**, *10*, S1484–S1491. [CrossRef]
9. Stanić, Z.; Girousi, S. Carbon Paste Electrodes in Potentiometry: The State of the Art and Applications in Modern Electroanalysis (A Review). In *Sensing in Electroanalysis*; University Press Centre: Pardubice, Czech Republic, 2011; Volume 6, ISBN 9788073954345.
10. Gupta, V.K.; Yola, M.L.; Özaltin, N.; Atar, N.; Üstündağ, Z.; Uzun, L. Molecular imprinted polypyrrole modified glassy carbon electrode for the determination of tobramycin. *Electrochim. Acta* **2013**, *112*, 37–43. [CrossRef]
11. Onac, C.; Kaya, A.; Yola, M.L.; Alpoguz, H.K. Determination of Tobramycin by Square Wave Voltammetry from Milk Sample through the Modified Polymer Inclusion Membrane with Reduced Graphene Oxide. *ECS J. Solid State Sci. Technol.* **2017**, *6*, M152–M155. [CrossRef]
12. Hadi, M.; Mollaei, T. Reduced graphene oxide/graphene oxide hybrid-modified electrode for electrochemical sensing of tobramycin. *Chem. Pap.* **2019**, *73*, 291–299. [CrossRef]
13. El-Kosasy, A.M. Potentiometric assessment of Gram-negative bacterial permeabilization of tobramycin. *J. Pharm. Biomed. Anal.* **2006**, *42*, 389–394. [CrossRef]
14. Kalcher, K. Chemically modified carbon paste electrodes in voltammetric analysis. *Electroanalysis* **1990**, *2*, 419–433. [CrossRef]
15. Afkhami, A.; Soltani-Felehgari, F.; Madrakian, T. Gold nanoparticles modified carbon paste electrode as an efficient electrochemical sensor for rapid and sensitive determination of cefixime in urine and pharmaceutical samples. *Electrochim. Acta* **2013**, *103*, 125–133. [CrossRef]
16. Da Silveira, J.P.; Piovesan, J.V.; Spinelli, A. Carbon paste electrode modified with ferrimagnetic nanoparticles for voltammetric detection of the hormone estriol. *Microchem. J.* **2017**, *133*, 22–30. [CrossRef]
17. Ghapanvari, M.; Madrakian, T.; Afkhami, A.; Ghoorchian, A. A modified carbon paste electrode based on Fe_3O_4@multi-walled carbon nanotubes@polyacrylonitrile nanofibers for determination of imatinib anticancer drug. *J. Appl. Electrochem.* **2020**, *50*, 281–294. [CrossRef]
18. Fekry, A.M. A new simple electrochemical Moxifloxacin Hydrochloride sensor built on carbon paste modified with silver nanoparticles. *Biosens. Bioelectron.* **2017**, *87*, 1065–1070. [CrossRef]
19. Lima, D.; Calaça, G.N.; Viana, A.G.; Pessôa, C.A. Porphyran-capped gold nanoparticles modified carbon paste electrode: A simple and efficient electrochemical sensor for the sensitive determination of 5-fluorouracil. *Appl. Surf. Sci.* **2018**, *427*, 742–753. [CrossRef]
20. Zhang, Z.; Shen, W.; Xue, J.; Liu, Y.; Liu, Y.; Yan, P.; Liu, J.; Tang, J. Recent advances in synthetic methods and applications of silver nanostructures. *Nanoscale Res. Lett.* **2018**, *13*, 54. [CrossRef] [PubMed]
21. Maduraiveeran, G.; Jin, W. Nanomaterials based electrochemical sensor and biosensor platforms for environmental applications. *Trends Environ. Anal. Chem.* **2017**, *13*, 10–23. [CrossRef]
22. Zdrachek, E.; Bakker, E. Potentiometric Sensing. *Anal. Chem.* **2019**, *91*, 2–26. [CrossRef] [PubMed]
23. Fu, L.; Wang, A.; Lai, G.; Lin, C.-T.; Yu, J.; Yu, A.; Liu, Z.; Xie, K.; Su, W. A glassy carbon electrode modified with N-doped carbon dots for improved detection of hydrogen peroxide and paracetamol. *Microchim. Acta* **2018**, *185*, 87. [CrossRef]
24. Bonet-San-Emeterio, M.; Algarra, M.; Petković, M.; Del Valle, M. Modification of electrodes with N-and S-doped carbon dots. *Evaluation of the electrochemical response. Talanta* **2020**, *212*, 120806. [CrossRef] [PubMed]
25. Sha, R.; Jones, S.S.; Vishnu, N.; Soundiraraju, B.; Badhulika, S. A Novel Biomass Derived Carbon Quantum Dots for Highly Sensitive and Selective Detection of Hydrazine. *Electroanalysis* **2018**, *30*, 2228–2232. [CrossRef]
26. Spanu, D.; Binda, G.; Dossi, C.; Monticelli, D. Biochar as an alternative sustainable platform for sensing applications: A review. *Microchem. J.* **2020**, *159*, 105506. [CrossRef]
27. Sun, X.; Lei, Y. Fluorescent carbon dots and their sensing applications. *TrAC Trends Anal. Chem.* **2017**, *89*, 163–180. [CrossRef]
28. Tajik, S.; Dourandish, Z.; Zhang, K.; Beitollahi, H.; Van Le, Q.; Jang, H.W.; Shokouhimehr, M. Carbon and graphene quantum dots: A review on syntheses, characterization, biological and sensing applications for neurotransmitter determination. *RSC Adv.* **2020**, *10*, 15406–15429. [CrossRef]
29. Ji, H.; Zhou, F.; Gu, J.; Shu, C.; Xi, K.; Jia, X. Nitrogen-doped carbon dots as a new substrate for sensitive glucose determination. *Sensors* **2016**, *16*, 630. [CrossRef] [PubMed]
30. Palakollu, V.N.; Karpoormath, R.; Wang, L.; Tang, J.N.; Liu, C. A versatile and ultrasensitive electrochemical sensing platform for detection of chlorpromazine based on nitrogen-doped carbon dots/cuprous oxide composite. *Nanomaterials* **2020**, *10*, 1513. [CrossRef]
31. Mongay, C.; Cerdra, V. A Britton-Robinson buffer of known ionic strangth. *Ann. Chim.* **1974**, *64*, 409–412.
32. Qu, S.; Wang, X.; Lu, Q.; Liu, X.; Wang, L. A biocompatible fluorescent ink based on water-soluble luminescent carbon nanodots. *Angew. Chemie* **2012**, *51*, 12215–12218. [CrossRef] [PubMed]
33. He, X.; Li, H.; Liu, Y.; Huang, H.; Kang, Z.; Lee, S.-T. Water soluble carbon nanoparticles: Hydrothermal synthesis and excellent photoluminescence properties. *Colloids Surfaces B Biointerfaces* **2011**, *87*, 326–332. [CrossRef]
34. De Medeiros, T.V.; Manioudakis, J.; Noun, F.; Macairan, J.-R.; Victoria, F.; Naccache, R. Microwave-assisted synthesis of carbon dots and their applications. *J. Mater. Chem. C* **2019**, *7*, 7175–7195. [CrossRef]
35. Jahanbakhshi, M.; Habibi, B. A novel and facile synthesis of carbon quantum dots via salep hydrothermal treatment as the silver nanoparticles support: Application to electroanalytical determination of H_2O_2 in fetal bovine serum. *Biosens. Bioelectron.* **2016**, *81*, 143–150. [CrossRef]

36. Newman Monday, Y.; Abdullah, J.; Yusof, N.A.; Abdul Rashid, S.; Shueb, R.H. Facile Hydrothermal and Solvothermal Synthesis and Characterization of Nitrogen-Doped Carbon Dots from Palm Kernel Shell Precursor. *Appl. Sci.* **2021**, *11*, 1630. [CrossRef]
37. Guo, Y.; Zhang, L.; Cao, F.; Leng, Y. Thermal treatment of hair for the synthesis of sustainable carbon quantum dots and the applications for sensing Hg^{2+}. *Sci. Rep.* **2016**, *6*, 35795. [CrossRef]
38. Kumar, V.B.; Borenstein, A.; Markovsky, B.; Aurbach, D.; Gedanken, A.; Talianker, M.; Porat, Z. Activated Carbon Modified with Carbon Nanodots as Novel Electrode Material for Supercapacitors. *J. Phys. Chem. C* **2016**, *120*, 13406–13413. [CrossRef]
39. Peterson, L.N. Inhibition of tobramycin reabsorption in nephron segments by metabolic alkalosis. *Kidney Int.* **1990**, *37*, 1492–1499. [CrossRef]
40. Jaworska, E.; Lewandowski, W.; Mieczkowski, J.; Maksymiuk, K.; Michalska, A. Simple and disposable potentiometric sensors based on graphene or multi-walled carbon nanotubes-Carbon-plastic potentiometric sensors. *Analyst* **2013**, *138*, 2363–2371. [CrossRef] [PubMed]
41. Hussein, L.A.; Magdy, N.; Yamani, H.Z. Stable glycopyrronium bromide solid contact ion selective potentiometric sensors using multi-walled carbon nanotubes, polyaniline nanoparticles and polyaniline microparticles as ion-to-electron transducers: A comparative study. *Sens. Actuators B Chem.* **2017**, *247*, 436–444. [CrossRef]
42. Shabani, R.; Rizi, Z.L.; Moosavi, R. Selective potentiometric sensor for isoniazid ultra-trace determination based on Fe_3O_4 nanoparticles modified carbon paste electrode (Fe_3O_4/CPE). *Int. J. Nanosci. Nanotechnol.* **2018**, *14*, 241–249.
43. Buck, R.P.; Lindner, E. Recomendations for nomenclature of ion-selective electrodes (IUPAC recommendations 1994). *Pure Appl. Chem.* **1994**, *66*, 2527–2536. [CrossRef]
44. Qi, L.; Jiang, T.; Liang, R.; Qin, W. Polymeric membrane ion-selective electrodes with anti-biofouling properties by surface modification of silver nanoparticles. *Sens. Actuators B Chem.* **2021**, *328*, 129014. [CrossRef]
45. Zhao, D.L.; Chung, T.S. Applications of carbon quantum dots (CQDs) in membrane technologies: A review. *Water Res.* **2018**, *147*, 43–49. [CrossRef] [PubMed]
46. Koulivand, H.; Shahbazi, A.; Vatanpour, V.; Rahmandoost, M. Novel antifouling and antibacterial polyethersulfone membrane prepared by embedding nitrogen-doped carbon dots for efficient salt and dye rejection. *Mater. Sci. Eng. C* **2020**, *111*, 110787. [CrossRef]
47. Nie, J.; Yuan, L.; Jin, K.; Han, X.; Tian, Y.; Zhou, N. Electrochemical detection of tobramycin based on enzymes-assisted dual signal amplification by using a novel truncated aptamer with high affinity. *Biosens. Bioelectron.* **2018**, *122*, 254–262. [CrossRef] [PubMed]
48. Tohda, K.; Dragoe, D.; Shibata, M.; Umezawa, Y. Studies on the matched potential method for determining the selectivity coefficients of ion-selective electrodes based on neutral ionophores: Experimental and theoretical verification. *Anal. Sci.* **2001**, *17*, 733–743. [CrossRef]
49. Fibbioli, M.; Morf, W.E.; Badertscher, M.; De Rooij, N.F.; Pretsch, E. Potential drifts of solid-contacted ion-selective electrodes due to zero-current ion fluxes through the sensor membrane. *Electroanalysis* **2000**, *12*, 1286–1292. [CrossRef]